Surface Composition of Fluorinated Poly(amide urethane) Block Copolymers by Electron Spectroscopy for Chemical Analysis

Hengzhong Zhuang,[†] Kacey Gribbin Marra,[‡] Tai Ho,[§] Toby M. Chapman,[‡] and Joseph A. Gardella Jr.*[,†]

Department of Chemistry, State University of New York at Buffalo, Buffalo, New York 14260, Department of Chemistry, University of Pittsburgh, Pittsburgh, Pennsylvania 15260, and Department of Chemistry, Virginia Polytechnic Institute and State University, Blacksburg, Virginia 24061

Received June 20, 1995; Revised Manuscript Received November 15, 1995[⊗]

ABSTRACT: The surface composition and near-surface depth profiles of annealed films of poly(amide urethane) block copolymers were measured using angle-dependent electron spectroscopy for chemical analysis (ESCA). Segregation of the fluorinated polyamide soft segment to the surface was detected and quantified. The poly(amide urethane)s were made from amine-terminated polyamides with N-alkylated fluorinated side chains as well as fluorinated backbones, methylenebis(cyclohexandiyl diisocyanate) (H_{12}-MDI), and butanediol.[1] The resulting copolymers display extremely low surface energy. A deconvolution program was utilized to obtain composition−depth profiles and to confirm phase segregation.

Introduction

The synthesis and characterization of low surface energy poly(amide urethane) block copolymers have been previously reported by the University of Pittsburgh group.[1] Analysis of contact angle measurements indicated a surface dominated by the fluorinated components; we are interested in further discerning the composition and morphology of the surface at the air−polymer interface. In the present work, angle-dependent electron spectroscopy for chemical analysis (ESCA) is employed, and the topmost 100 Å of annealed films has been examined.

Since photoelectron intensities detected by ESCA are convoluted signals—i.e., all atoms in the path of the X-ray contribute to the signal[2]—deconvolution methods must be used to obtain composition−depth profiles. Such methods have been employed by several research groups, including a method of regularization by Ratner *et al.*[3] used to analyze polymers and several different deconvolution algorithms introduced and compared by Fulghum *et al.* for the determination of overlayer thicknesses and/or concentration gradients.[4] The present work utilizes a recently developed numerical method that simulates depth profiles of the individual components in a block copolymer by introducing boundary conditions based on the composition.[5]

The series of fluorinated polyamides and their corresponding poly(amide urethane) block copolymers described in structures **1** and **2**, along with Tables 1 and 2, were studied. The present work focuses on samples which have been annealed to attain a thermodynamic equilibrium. Since fluorocarbons display very low surface energy, these poly(amide urethane)s would be expected to have a low energy surface if there was microphase separation. Previous work reported contact angle measurements and determined critical surface tensions as low as 11 dyn/cm;[1] therefore, such phase segregation was suspected. The low energy surface properties of these copolymers make them potential candidates for minimal-fouling coating applications.[6,7]

Table 1. Four Different Polyamides and Their Code Names

	n	*m*	total no. of fluorines per repeat unit	code name
1a	*a*	3	0	0F−6F
1b	1	3	5	5F−6F
1c	1	4	5	5F−8F
1d	6	3	15	15F−6F

[a] Prepared with a nonfluorinated propyl side chain.

Table 2. Four Different Poly(amide urethane)s and Their Code Names

	n	*m*	total no. of fluorines per repeat unit of polyamide blocks	code name	wt % polyamide
2a	*a*	3	0	0F−6F−HB[b]	44
2b	1	3	5	5F−6F−HB	45
2c	1	4	5	5F−8F−HB	30
2d	6	3	15	15F−6F−HB	37

[a] Prepared with nonfluorinated propyl side chain. [b] H = H_{12}MDI and B = butanediol.

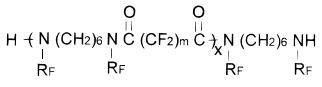

1

where R_F=$CH_2(CF_2)_nCF_3$

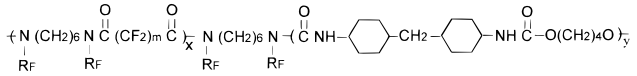

2

where R_F=$CH_2(CF_2)_nCF_3$

Experimental Section

Sample Preparation. The preparation of the poly(amide urethane) block copolymers has been previously described.[1] The structures of the copolymers are shown in structures **1** and **2**, with their compositions and code names given in Tables 1 and 2.

The films of the polymers were prepared by casting 0.2−2.0% solutions from 1,1,1,3,3,3-hexafluoro-2-propanol (HFIP) or the mixed solvents of dimethylacetamide and tetrahydrofuran onto aluminum foil. The films were annealed in an

* Author to whom correspondence should be addressed.
[†] State University of New York at Buffalo.
[‡] University of Pittsburgh.
[§] Virginia Polytechnic Institute and State University.
[⊗] Abstract published in *Advance ACS Abstracts,* February 1, 1996.

0024-9297/96/2229-1660$12.00/0

Scheme 1. Proposed Surface Structure of the Poly(amide urethane)s

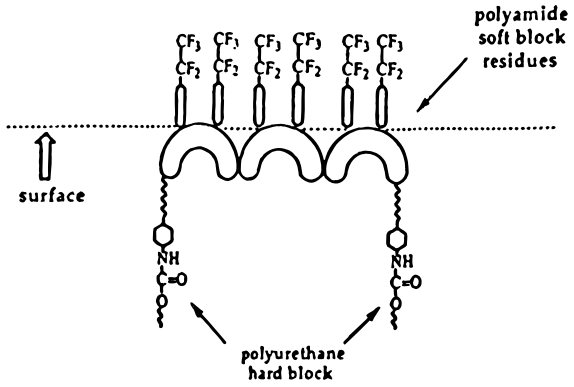

Abderhalden pistol for 48−72 h at several degrees above their glass transition temperatures.[1] Ultrasonic extraction of the films in hexane did not produce significant differences in ESCA measurements. Thus, evanescent surface impurities can be eliminated as a contribution to the results.

Instrumentation. Angle-dependent ESCA data were obtained using a Physical Electronics (PHI) Model 5100 spectrometer equipped with a Mg/Ti dual-anode source and an Al/Be window. The system uses a hemispherical analyzer with a single-channel detector. Mg Kα X-rays (1253.6 eV) were used as an achromatic source, operated at 300 W (15 kV and 20 mA). The base pressure of the system was lower than 5×10^{-9} Torr, with an operating pressure no higher than 1×10^{-7} Torr. A pass energy of 89.45 eV was used when obtaining the survey spectra, and a pass energy of 35.75 eV was used for the high-resolution spectra of elemental regions. Spectra were obtained at the following take-off angles: 10, 15, 30, and 90°. The instrument was calibrated using Mg Kα X-radiation: the distance between Au $4f_{7/2}$ and Au $4f_{5/2}$ was 3.65 eV, the distance between Au $4f_{7/2}$ and Cu $2p_{3/2}$ was set at 848.67 eV, and the work function was set using Au $4f_{7/2}$ and Cu $2p_{3/2}$ and checked using Au $3d_{5/2}$. All metals were sputter cleaned to remove oxides. Full width at half-maximum for Ag $3d_{3/2}$ was measured to be 0.8 eV at a count rate of 30 000 counts.

ESCA Data Calculations. With the sensitivity factors provided in the software supplied by PHI and verified by Vargo and Gardella[8] using polymer standards, the peak area integration and subsequent composition calculation (atomic percentages) were performed using a Perkin-Elmer 7500 professional computer running PHI ESCA Version 2.0 software. From the atomic percentages, composition−depth profiles were achieved using the following protocol.

In the previous work using the numerical method,[5,9] the poly(dimethylsiloxane urethane) (PDMS−PU) segmented copolymer chains are divided into soft and hard segments. Since nitrogen is unique to the hard segments, the weight percentage of PDMS (soft segment) or polyurethane (hard segment) can be calculated from the atomic ratio of nitrogen to carbon (N/C).[5] In the present work, the poly(amide urethane) copolymers can be similarly divided into soft and hard blocks. However, it could be misleading to use fluorine to represent the entire soft block in the copolymer with long fluorinated side chains, particularly in the case of copolymer 15F−6F−HB.

In copolymer 15F−6F−HB, much of the fluorine is contained in the side chain. Therefore, the long side chains would expectedly orient toward the air−polymer interface due to their lower surface energy when the copolymer is solution-cast into films (see Scheme 1). In other words, the side chains and the backbones in the same soft block could position at different depths with the side chains closer to the surface. Consequently, if one uses fluorine to label the whole soft block, one would inevitably "locate" the soft block, especially the backbones, at a shallower depth than the actual. The resulting profile of the soft block concentrations versus sampling depths would deviate. This possibility prompted us to determine the concentration−depth profile of CF_x (representing CF_2 and CF_3) segments instead.

Table 3. Values of *C*, *η*, *σ*, and *γ* Used in Recovering the Concentration Profiles of CF_x

copolymers	*C*	*η*	*σ*	*γ*
0F−6F−HB	0.163	40.00	54.48	2.00
5F−6F−HB	0.319	18.04	57.82	2.29
5F−8F−HB	0.220	18.26	56.53	2.25
15F−6F−HB	0.314	19.14	57.15	2.12

The principle of revealing the concentration−depth profile of CF_x is the same as that described in ref 5. The intensities of the photoelectronic response from fluorine and carbon atoms as functions of the take-off angles can be formulated as

$$dI_F(\theta) = F\alpha_F N_F(x) K e^{-x/(\lambda_F \sin\theta)}\, dx \quad (1)$$

$$dI_C(\theta) = F\alpha_C N_C(x) K e^{-x/(\lambda_C \sin\theta)}\, dx \quad (2)$$

where *I* is the detected intensity of photoelectrons from a given atom, subscripts F and C denote fluorine and carbon, respectively, θ is the take-off angle, *F* is the X-ray flux, α is the cross-section of photoionization in a given shell of a given atom for a given X-ray energy, $N(x)$ is the depth profile of the atomic density, *x* is the vertical distance from the free surface, *K* is a spectrometer factor, and λ is the escape depth of the electrons.

For convenience, assuming *F*, α, and *K* are independent of *x* and defining normalized intensity $I'(\theta)$ as $I(\theta)/(F\alpha K)$, one can integrate eqs 1 and 2 and obtain

$$I_F'(\theta) = I_F(\theta)/(F\alpha_F K) = \int_0^\infty N_F(x) e^{-x/(\lambda_F \sin\theta)}\, dx \quad (3)$$

$$I_C'(\theta) = I_C(\theta)/(F\alpha_C K) = \int_0^\infty N_C(x) e^{-x/(\lambda_C \sin\theta)}\, dx \quad (4)$$

or

$$I_F'(\theta)/I_C'(\theta) = [\int_0^\infty N_F(x) e^{-x/(\lambda_F \sin\theta)}\, dx]/[\int_0^\infty N_C(x) e^{-x/(\lambda_C \sin\theta)}\, dx] \quad (5)$$

Normalized intensities for different atoms at a take-off angle θ, usually reported as a ratio, such as I_F'/I_C', can be obtained from the ESCA data.

As mentioned previously, the polymer chains were divided into the CF_x component and the non-CF_x component. The weight fraction (*C*) of CF_x segments, the number density (η) of carbon atoms in CF_x segments, the number density (σ) of carbon atoms in the non-CF_x component, and the atomic ratio (γ) of *F*/*C* in CF_x segments for different copolymers were calculated and summarized in Table 3.

To facilitate the understanding of the above definitions and their calculations, a set of sample calculations of the values of *C*, η, σ, and γ for 15F−6F−HB copolymer is given explicitly as follows:

C = (wt % polyamide) × (MW of CF_x segments in one repeat unit of the soft block)/(MW of one repeat unit of the soft block)

$= 37\% \times 888/1048$

$= 0.314$

η = (no. of carbons in CF_x segments) × 10^3/(MW of CF_x segments in one repeat unit of the soft block)

$= 17 \times 10^3/888$

$= 19.14\ [L^{-1}]$

σ = (no. of carbons in the non-CF_x component) × 10^3/(MW of the non-CF_x component)

= (19/352) × 63% × 10^3 + [10/(1048 − 888)] × 37% × 10^3

= 57.15 [L^{-1}]

γ = (no. of fluorines in CF_x segments)/(no. of carbons in CF_x segments)

= 36/17

= 2.12

Given that $\nu(x)$ is the depth profile of CF_x segments (i.e., the volume fractions of CF_x segments as a function of sampling depth), atomic depth profiles for fluorine and carbon can be derived as eqs 6 and 7, assuming the difference between weight fraction and volume fraction values is negligible.

$$N_C(x) = \eta\nu + \sigma(1 - \nu) \quad (6)$$

$$N_F(x) = \eta\nu\gamma \quad (7)$$

Then, eqs 6 and 7 are inserted into eq 5, giving

$$I_F'(\theta)/I_C'(\theta) = [\int_0^\infty \eta\nu(x)\gamma e^{-x/(\lambda_F \sin\theta)}\, dx]/[\int_0^\infty ((\eta\nu(x) + \sigma(1 - \nu(x)))e^{-x/(\lambda_C \sin\theta)}\, dx] \quad (8)$$

So far, the only variation except x on the right-hand side of eq 8 is $\nu(x)$. If $\nu(x)$ is known, $I_F'(\theta)/I_C'(\theta)$ can be calculated, although, in reality, $I_F'(\theta)/I_C'(\theta)$ (see Table 5), instead of $\nu(x)$, is readily available.

In this work, we constructed a mathematical equation (eq 9) with five variables to simulate $\nu(x)$ in eq 8.

$$\nu(x) = 1 - H \exp[-0.5(x - X)^2/S_1^2](1 - C) \quad x \le X$$
$$= 1 - \{b + (H - b)\exp[-0.5(x - X)^2/S_2^2]\} \times (1 - C) \quad x > X \quad (9)$$

where $\nu(x)$ is the volume fraction of CF_x segments, H is a parameter relevant to the magnitude of the trough on the profile, x is the distance from the surface (in angstroms), X is the location of the trough of the profile, S_1 characterizes the shape of the profile to the left of the trough, S_2 characterizes the shape of the profile to the right of the trough, C is the volume fraction of CF_x segments in the bulk (again, assuming the difference between weight fraction and volume fraction values is negligible), and b evaluates the height of the plateau in the profile.

The ratio of the detected intensities of photoelectrons from fluorine and carbon, designated as R, can be calculated using eq 9 through adjusting the five variables and compared with experimental values.

To reach optimal values for the variables, the following objective function was used.

$$\psi = \{(1/n)\sum[[R_{cal}(H,X,S_1,S_2,b) - R_{exp}(\theta_n)]/R_{exp}(\theta_n)]^2\}^{1/2} \quad (10)$$

where n is the number of take-off angles. The optimization was achieved using the algorithm developed by Dr. Tai Ho and programmed in Mathcad 5.0.

Upon data fitting, the influence of the different inelastic mean free paths (IMFP) for C_{1s} and F_{1s} electrons was considered and corrected. The IMFPs for C_{1s} and F_{1s} were calculated with the modified Bethe[10] equation since the Seah−Dench[11] equation tends to overestimate the IMFP in the low-energy region while underestimating the IMFP in the high-energy region.[10] The resultant IMFPs of C_{1s} electrons are 30 Å for copolymers 0F−6F−HB, 5F−6F−HB, and 5F−8F−HB (see Scheme 1 for chemical structures) with estimated densities[12] of 1.14, 1.27, and 1.22 g/cm^3, respectively, and 28 Å for copolymer 15F−6F−HB with an estimated density of 1.29 g/cm^3. The IMFPs of F_{1s} electrons are 20 Å for copolymers 0F−6F−HB, 5F−6F−HB, and 5F−8F−HB and 18 Å for copolymer 15F−6F−HB.

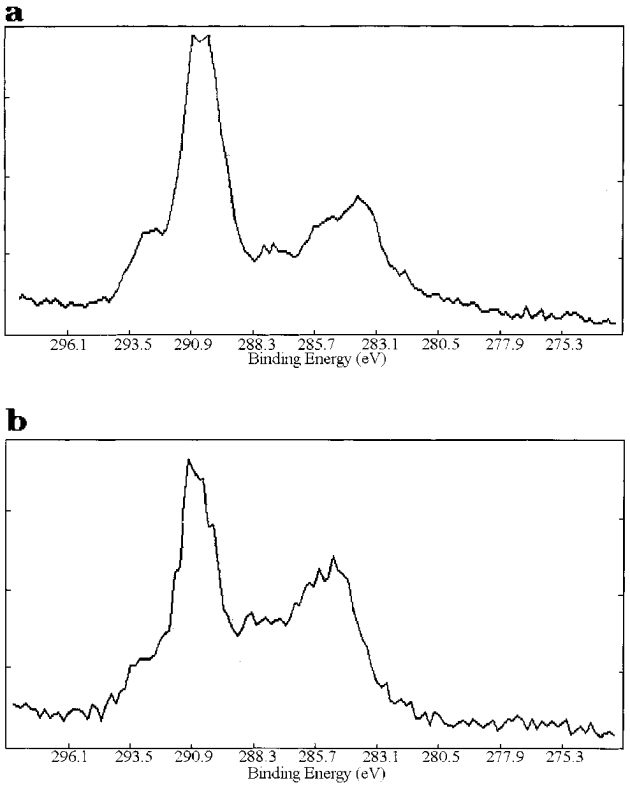

Figure 1. ESCA spectra of copolymer 15F−6F−HB in the C_{1s} region recorded at (a) 10° take-off angle and (b) 90° take-off angle.

Results and Discussion

In ESCA, there are two ways to evaluate the composition in the near-surface region, i.e., elemental analysis and curve fitting.[13] In this case, one could use elemental analysis of fluorine, which can be quantitatively related to the soft block, and/or the analysis of the intensity of the chemical shift due to the CF_x fraction of functional groups containing carbon.[13] For the latter approach, a typical ESCA C_{1s} spectrum for copolymer 15F−6F−HB at 10° take-off angle is shown in Figure 1a. The large peak at ∼290.5 ± 0.1 eV represents fluorocarbons, the small middle peak represents carbonyl carbons, and the peak at ∼285.0 ± 0.1 eV identifies the hydrocarbons. The dominance of the C_{1s} peak at ∼290.5 ± 0.1 eV indicates a large concentration of fluorinated polyamide soft block at the surface. In comparison with Figure 1a, the C_{1s} spectrum for copolymer 15F−6F−HB at 90° take-off angle is shown in Figure 1b, in which the amount of hydrocarbon has grown relative to fluorocarbon. It suggests that the concentration of fluorinated polyamide soft block at 10° take-off angle is higher than that at 90°. In other words, the information from the C_{1s} region does show a trend of the concentration gradient of fluorinated polyamide soft blocks in the surface region. However, quantitative analysis using curve fitting is not convenient because the inexact knowledge of the binding energies of the functional groups with fluorine and oxygen present makes curve fitting in the C_{1s} region difficult.[14]

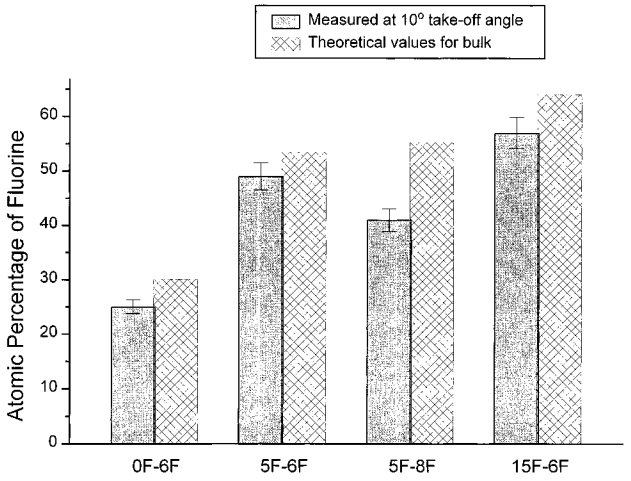

Figure 2. Atomic percentages of fluorine for polyamides; data taken at 10°.

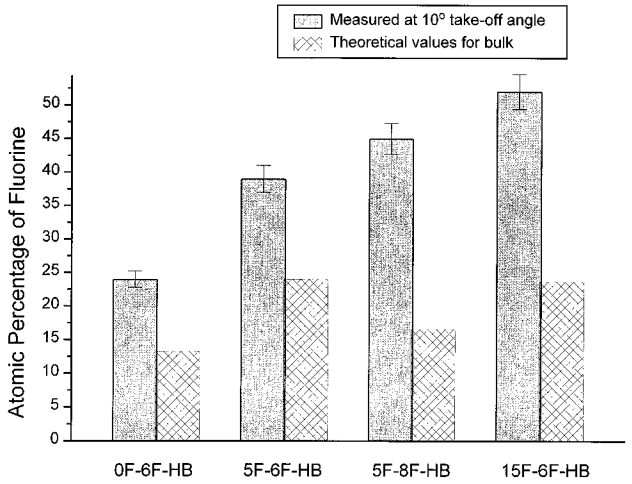

Figure 3. Atomic percentages of fluorine for poly(amide urethane)s; data taken at 10°.

Table 4. Atomic Percentage of Fluorine in the Polymers (±5%), Determined by Angle-Dependent ESCA, As Reflected by Peak Ratios Prior to Deconvolution

	take-off angle				theoretical
polymer	10°	15°	30°	90°	% F
0F−6F	25 ± 1	25 ± 1	20 ± 1	21 ± 1	30.14
5F−6F	49 ± 3	49 ± 3	43 ± 2	43 ± 2	53.50
5F−8F	41 ± 2	42 ± 2	39 ± 2	40 ± 2	55.31
15F−6F	57 ± 3	55 ± 3	43 ± 2	44 ± 2	64.03
0F−6F−HB	24 ± 1	21 ± 1	18 ± 1	16 ± 1	13.26
5F−6F−HB	39 ± 2	36 ± 2	32 ± 1	27 ± 1	24.07
5F−8F−HB	45 ± 2	44 ± 2	42 ± 1	38 ± 2	16.59
15F−6F−HB	52 ± 3	51 ± 3	49 ± 3	43 ± 2	23.69

Alternatively, atomic percentages of fluorine (% F) were obtained from elemental analysis of ESCA results. Table 4 lists the % F's for polyamides 0F−6F, 5F−6F, 5F−8F, and 15F−6F (see Structure **1** and Table 1 for chemical structures) and those for poly(amide urethane)s 0F−6F−HB, 5F−6F−HB, 5F−8F−HB, and 15F−6F−HB at four take-off angles.

Interestingly, the % F's for the polyamides in Table 4 and Figure 2 are slightly, but consistently, lower than the calculated bulk or average values. We expected that the values would be equivalent to bulk values since no phase separation is expected in these samples. As discussed previously, the IMFP for F_{1s} electrons is smaller than not only that for C_{1s} electrons but also those for O_{1s} and N_{1s} electrons. Consequently, in the calculation of atomic percentages at a particular angle, the signal intensity from F will be underestimated; on the other hand, the signal intensities for C, O, and N will be relatively overestimated, thereby resulting in lower surface % F's for polyamides than the theoretical bulk % F's. This serves well as direct experimental evidence, prompting us to factor the IMFP in the later depth profile calculations.

Of the two components in poly(amide urethane)s, the fluorinated polyamide (soft block) has a lower surface energy than the polyurethane (hard block). Thus, we expect this soft block to segregate at the air−polymer interface. The ESCA results in Table 4 and Figure 3 support this model. Even though they were underevaluated due to the shorter IMFP of F_{1s} electrons, the measured % F's were still significantly (95% confidence level) higher than the bulk % F's at four take-off angles for all the poly(amide urethane)s, and the % F's for the poly(amide urethane)s decrease from the air−polymer interface to the bulk, consistent with the conclusion drawn from the comparison of spectra a and b of Figure 1. In addition, the % F's at four take-off angles listed in Table 4 for the poly(amide urethane)s are close to those for the corresponding polyamides. This similarity suggests that there is a phase segregation so that the polyamide is coating the poly(amide urethane) block.

The extent of surface segregation of the fluorinated component strongly depends on the structure of the fluorinated poly(amide urethane)s and the bulk composition. As shown in Figure 3, copolymer 5F−6F−HB yielded a higher surface % F than 0F−6F−HB as a result of a higher percentage of the fluorinated component in the bulk and fluorinated side chain (see structure **2** and Table 2 for structure information). Copolymer 5F−8F−HB displayed a substantially higher surface % F than copolymer 5F−6F−HB although the latter has a higher bulk % F than the former. This observation could be attributed to "bending" toward the surface of the longer fluorinated segments in the backbone of copolymer 5F−8F−HB. It is of particular interest to compare copolymer 5F−6F−HB with copolymer 15F−6F−HB. Copolymer 15F−6F−HB displayed a remarkably higher % F than copolymer 5F−6F−HB even though they have almost the same bulk % F. As illustrated in structure **2** and Table 2, there are long fluorinated side chains in copolymer 15F−6F−HB. When the poly(amide urethane)s were solution-cast into a film, it was expected that the low surface energy fluorinated moieties would migrate and perhaps orient toward the surface on solvent evaporation, forming a surface morphology depicted (or schematically illustrated) in Scheme 1.[1] Therefore, the longer the fluorinated side chain, the higher the surface % F expected.

As it is, in ESCA measurements, photoelectron intensities detected are convoluted signals; i.e., all atoms within the path of the probing X-ray contribute to the signal but the contribution of each decreases exponentially with the distance from the free surface.[2] The convoluted nature of the angle-dependent measurements distorts depth profiles for samples with compositional gradients. To recover the true depth profiles for such samples from atomic percentages of carbon and fluorine listed in Table 5, the modified deconvolution method, described above, was utilized.[5]

In contrast to the angle-dependent ESCA data in Table 4, which merely suggest a monotonic increase of the hard block, or a monotonic decrease of the fluorinated polyamide (soft block), from the surface to the

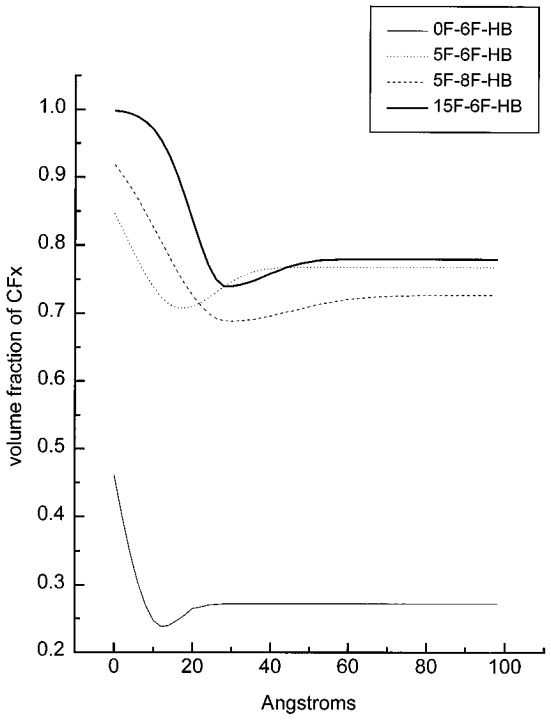

Figure 4. Concentration depth profiles for poly(amide urethane)s.

Table 5. Atomic Percentage of Carbon, Oxygen, and Nitrogen in the Poly(amide urethane) (±5%) Prior to Deconvolution

		take-off angle				
polymer		10°	15°	30°	90°	theoretical
0F−6F−HB	% C	58 ± 3	58 ± 3	56 ± 3	52 ± 3	63.68
	% O	11 ± 1	13 ± 1	18 ± 1	25 ± 1	14.91
	% N	7 ± 0	7 ± 0	8 ± 0	7 ± 0	8.15
	% F	24 ± 1	22 ± 1	18 ± 1	16 ± 1	13.26
5F−6F−HB	% C	44 ± 2	44 ± 2	41 ± 2	36 ± 2	55.38
	% O	13 ± 1	15 ± 1	22 ± 1	33 ±2	13.52
	% N	4 ± 0	5 ± 0	5 ± 0	4 ± 0	7.03
	% F	39 ± 2	36 ± 2	32 ± 1	27 ± 1	24.07
5F−8F−HB	% C	44 ± 2	45 ± 2	47 ± 2	50 ± 3	60.40
	% O	5 ± 0	5 ± 0	5 ± 0	7 ± 0	15.53
	% N	6 ± 0	6 ± 0	6 ± 0	5 ± 0	7.48
	% F	45 ± 2	44 ± 2	42 ± 1	38 ± 2	16.59
15F−6F−HB	% C	39 ± 0	43 ± 2	43 ± 2	48 ± 2	56.14
	% O	5 ± 0	4 ± 0	5 ± 0	5 ± 0	13.69
	% N	4 ± 0	2 ± 0	3 ± 0	4 ± 0	6.48
	% F	52 ± 3	51 ± 3	49 ± 3	43 ± 2	23.69

bulk, Figure 4 displays the recovered in-depth concentration profiles for copolymers 0F−6F−HB, 5F−6F−HB, 5F−8F−HB, and 15F−6F−HB. These results show segregation or surface excess regions of the soft block in the topmost layer followed immediately by the depletion regions. This latter feature of the concentration−depth profile cannot be measured directly with existing techniques. A reasonable explanation for this feature is that the composition of the soft block integrated over one polymer chain length must equal its bulk composition (a constraint in our calculations). Therefore, any surface excess layer of the soft block must necessarily be followed by a depletion layer and vice versa.

First, from these profiles an extrapolated "surface composition" ($x = 0$) can be determined and compared. Volume fractions (ν_{CF_x}) of CF_x segments at the very top surface ($x = 0$) for copolymers 15F−6F−HB, 5F−8F−HB, and 5F−6F−HB are 0.998, 0.919, and 0.847, respectively, while that for copolymer 0F−6F−HB is 0.461. This follows the same trend as the 10° ESCA data in Figure 3.

Second, as two important factors characterizing the depletion zone (the trough), the depth from the surface (i.e., the thickness of the surface excess layer) and the magnitude (y value) can be evaluated. The depths of the depletion regions for copolymers 15F−6F−HB, 5F−8F−HB, 5F−6F−HB, and 0F−6F−HB are 26, 29, 17, and 12 Å from the surface. As discussed earlier, poly(amide urethane)s with long fluorinated side chains favor forming a thicker fluorine-rich layer in the surface region upon solvent evaporation when solution-cast into films. However, copolymer 0F−6F−HB does not have such luxury, and a thinner fluorine-rich topmost layer was observed. The magnitudes of the trough in the profiles for copolymers 15F−6F−HB, 5F−8F−HB, and 5F−6F−HB are 0.740, 0.688, and 0.708, respectively, while that for copolymer 0F−6F−HB is 0.238. These values, 0.740, 0.688, 0.708, and 0.238, roughly correlated with the bulk % F's, 23.69, 16.59, 24.07, and 13.26, of the copolymers.

The other specific comparisons can be made with these data. Among the poly(amide urethane)s with fluorinated side chains, copolymers 5F−8F−HB and 5F−6F−HB have the same fluorinated side chain, but their backbones differ, as shown in structure **2** and Table 2. As a result, copolymer 5F−8F−HB gives rise to a higher surface concentration of CF_x segments ($\nu_{CF_x} = 0.919$). Furthermore, the trough of the depletion region for copolymer 5F−8F−HB locates at 29 Å while that for copolymer 5F−6F−HB locates at 17 Å. This indicates the existence of a much thicker fluorine-rich layer in the surface region of copolymer 5F−8F−HB, due to the more readily "bending" of the fluorinated backbone in copolymer 5F−8F−HB toward the surface.

Copolymers 15F−6F−HB and 5F−6F−HB have the same backbone, but the length of their fluorinated side chains is different. As shown in Figure 4, copolymer 15F−6F−HB exhibits a significantly higher surface concentration of CF_x segments ($\nu_{CF_x} = 0.998$) and a much thicker fluorine-rich layer (26 Å) in the surface region, although it has almost the same bulk % F as copolymer 5F−6F−HB.

Although copolymer 15F−6F−HB gives rise to higher surface concentration of CF_x segments, $\nu_{CF_x} = 0.998$ ($x = 0$), than copolymer 5F−8F−HB, the thickness of the fluorine-rich surface layer for the former (26 Å) is equivalent (within error limits) to that for the latter (29 Å). This puzzling observation may be attributed to the "bending" of the fluorinated backbone in copolymer 5F−8F−HB toward the surface, further thickening the fluorine-rich surface layer.

Conclusions

Surface segregation was observed for poly(amide urethane) block copolymers. Higher concentrations of surface segregation were discerned for those poly(amide urethane)s with fluorinated side chains.

The composition−depth profiles extracted via a numerical deconvolution method further demonstrated the phase separation of the hard and soft blocks in the copolymer. They demonstrate that poly(amide urethane)s with fluorinated side chains form higher surface concentrations of CF_x segments and thicker fluorine-rich surface layers. The molecular structures of the

poly(amide urethane)s with fluorinated side chains have a profound influence on the composition−depth profiles.

Acknowledgment. This research was supported by grants to T.M.C. and J.A.G. from the Office of Naval Research, Molecular Interactions at Marine Interface Program.

References and Notes

(1) Chapman, T. M.; Marra, K. G. *Macromolecules* **1995**, *28*, 2081−2085. See also: Chapman, T. M.; Marra, K. G.; Benrashid, R.; Keener, J. P. *Macromolecules* **1995**, *28*, 331−336.
(2) Clark, D. T. *Adv. Polym. Sci.* **1977**, *24*, 126.
(3) Tyler, B. J.; Castner, D. G.; Ratner, B. D. *Surf. Interface Anal.* **1989**, *14*, 443.
(4) Tielsch, B. J.; Fulghum, J. E. *Surf. Interface Anal.* **1994**, *21*, 621−630.
(5) Ho, T.; Chen, X.; Gardella, J. A., Jr.; Wynne, K. J. *Macromolecules* **1995**, *28*, 1635−1642.
(6) Brady, R. F.; Griffith, J. R.; Love, K. S.; Field, D. E. *J. Coat. Technol.* **1987**, *59* (755), 133.
(7) Ho, T.; Wynne, K. J. *Macromolecules* **1992**, *25*, 3521.
(8) Vargo, T. G.; Gardella, J. A., Jr. *J. Vac. Sci. Technol.* **1989**, *A7* (3), May/June, 1733−1741.
(9) Gardella, J. A., Jr.; Ho, T.; Wynne, K. J.; Zhuang, H. *J. Colloid Interface Sci.* **1995**, *176*, 277−279.
(10) Tanuma, S.; Powell, C. J.; Pen, D. *Surf. Interface Anal.* **1993**, *21*, 165−176.
(11) Seah, M. P.; Dench, W. A. *Surf. Interface Anal.* **1979**, *1* (1), 2−11.
(12) Brandrup, J.; Immergut, E. H. *Polymer Handbook*, 3rd ed.; John Wiley & Sons: New York, 1989.
(13) Schmidt, J. J.; Gardella, J. A., Jr.; Salvati, L., Jr. *Macromolecules* **1989**, *22*, 4489.
(14) Vargo, T. G.; Gardella, J. A., Jr. *J. Polym. Sci., Part A: Polym. Chem.* **1991**, *29* (4), 555−570.

MA950860D